Journal of Geophysical Research-Solid Earth

Supporting Information for

Reduced lattice thermal conductivity of Fe-bearing bridgmanite in Earth's deep mantle

Wen-Pin Hsieh[1]*, Frédéric Deschamps[1], Takuo Okuchi[2], and Jung-Fu Lin[3]*

[1]*Institute of Earth Sciences, Academia Sinica, Nankang, Taipei 11529, Taiwan*

[2]*Institute for Planetary Materials, Okayama University, 827 Yamada, Misasa, Tottori, 682-0193 Japan*

[3]*Department of Geological Sciences, Jackson School of Geosciences, University of Texas at Austin, Austin, Texas 78712-0254, USA*

Contents of this file

SUPPLEMENTARY TABLE AND FIGURES

Table S1. Influence of the temperature exponent *n* (Eqs. (1) and (2)) on thermal conductivity and CMB heat flux. Listed parameters are root mean square (*rms*), minimum, and maximum in thermal conductivity and heat flux relative anomalies, and q^* parameter.

Quantity	*n*	*rms*	minimum	maximum	q*
Thermal conductivity anomalies					
$d\ln\Lambda^T$	0.5	0.0304	-0.0560	0.0793	-
$d\ln\Lambda^T$	1.0	0.0608	-0.1121	0.1585	-
$d\ln\Lambda$	0.5	0.1455	-0.3784	0.2469	-
$d\ln\Lambda$	1.0	0.1512	-0.3874	0.2882	-
Heat flux anomalies					
$d\ln\Phi^T = -dT/\Delta T_{ref} + d\ln\Lambda^T$	0.5	0.2739	-0.5043	0.7134	0.61
$d\ln\Phi^T = -dT/\Delta T_{ref} + d\ln\Lambda^T$	1.0	0.3044	-0.5603	0.7927	0.68
$d\ln\Phi$	0.5	0.2943	-0.4921	0.7651	0.63
$d\ln\Phi$	1.0	0.3211	-0.5177	0.8395	0.68

Thermal conductivity anomalies due to changes in temperature ($d\ln\Lambda^T$) are given by Eq. (2). Heat flux variations due to anomalies in temperature ($d\ln\Phi^T$) are given by the sum of the first and second terms in the right hand side of Eq. (14), $-dT(\varphi,\theta)/\Delta T_{ref} + d\ln\Lambda^T$. Total anomalies in thermal conductivity and heat flux, $d\ln\Lambda$ and $d\ln\Phi$, include the variations in conductivity due to composition, which do not depend on *n* and are similar to those in Table 2. The CMB temperature is fixed to T_{CMB} = 3750 K, the reference temperature and composition are T_{ref} = 3000 K (leading to ΔT_{ref} = 750 K), $X_{Bm,ref}$ = 0.8, $X_{Fe,ref}$ = 0.09, and the iron partitioning is set to K_D = 0.25. Calculations are made at lowermost mantle pressure, P = 120 GPa.

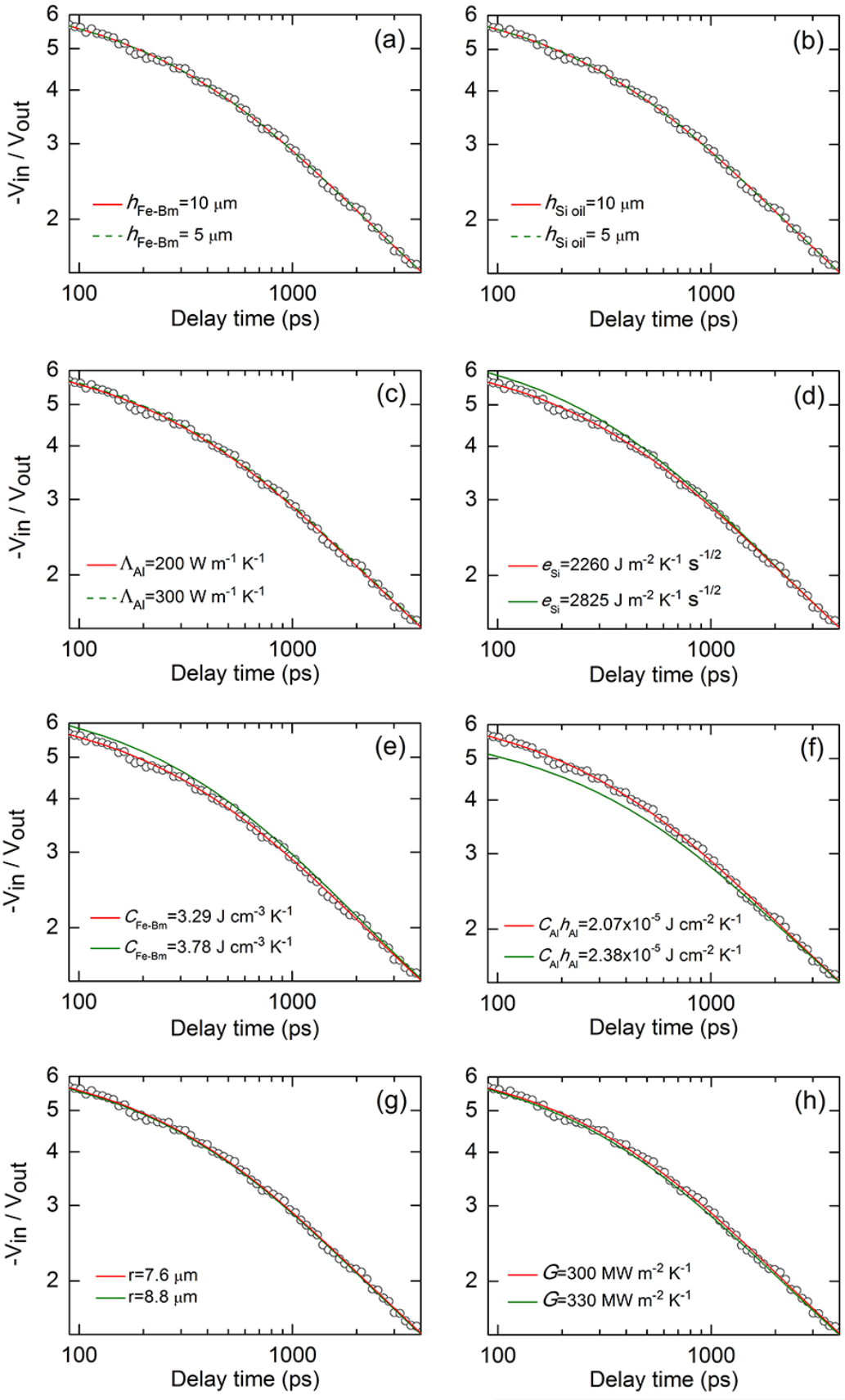
(a)
$h_{Fe\text{-}Bm}$=10 μm
$h_{Fe\text{-}Bm}$= 5 μm
(b)
$h_{Si\ oil}$=10 μm
$h_{Si\ oil}$= 5 μm
(c)
Λ_{Al}=200 W m^{-1} K^{-1}
Λ_{Al}=300 W m^{-1} K^{-1}
(d)
e_{Si}=2260 J m^{-2} K^{-1} s$^{-1/2}$
e_{Si}=2825 J m^{-2} K^{-1} s$^{-1/2}$
(e)
$C_{Fe\text{-}Bm}$=3.29 J cm^{-3} K^{-1}
$C_{Fe\text{-}Bm}$=3.78 J cm^{-3} K^{-1}
(f)
$C_{Al}h_{Al}$=2.07x10^{-5} J cm^{-2} K^{-1}
$C_{Al}h_{Al}$=2.38x10^{-5} J cm^{-2} K^{-1}
(g)
r=7.6 μm
r=8.8 μm
(h)
G=300 MW m^{-2} K^{-1}
G=330 MW m^{-2} K^{-1}
-Vin / Vout
Delay time (ps)
100
1000
2
3
4
5
6

Figure S1. Tests of the sensitivity of the thermal model to input parameters for Fe-Bm at 120 GPa. Here we fix the Fe-Bm thermal conductivity $\Lambda_{Fe\text{-}Bm}$ to be 14.5 W m^{-1} K^{-1} using parameters listed in Table 1. (a) and (b) A 50% decrease in the thicknesses of Fe-Bm ($h_{Fe\text{-}Bm}$) and silicone oil ($h_{Si\ oil}$), respectively, shows identical fits to the data, indicating uncertainties in their thicknesses do not influence the derived $\Lambda_{Fe\text{-}Bm}$. (c) Since the thermal conductivity of Al film, Λ_{Al}, is large, it has no effect on the $\Lambda_{Fe\text{-}Bm}$. (d) An example change of 25% thermal effusivity of the pressure medium silicone oil, $e=(\Lambda_{Si}C_{Si})^{1/2}$, deviates the model fit from the data, which requires a decrease of $\Lambda_{Fe\text{-}Bm}$ from 14.5 to 13.2 W m^{-1} K^{-1} to fit the data, i.e., approximately only 9% uncertainty to the $\Lambda_{Fe\text{-}Bm}$. (e) An uncertainty of 15% in the volumetric heat capacity of Fe-Bm, $C_{Fe\text{-}Bm}$, (3.29 to 3.78 J cm^{-3} K^{-1}), would require $\Lambda_{Fe\text{-}Bm}$ to decrease slightly to 12.6 W m^{-1} K^{-1} to fit the data, i.e., propagating only 13% uncertainty to the $\Lambda_{Fe\text{-}Bm}$. (f) Effect of the Al heat capacity per unit area, product of volumetric heat capacity and thickness, $C_{Al}\,h_{Al}$. The ratio $-V_{in}/V_{out}$ at few hundred ps delay time scales inversely with $C_{Al}\,h_{Al}$ [*Zheng et al.*, 2007]. An example uncertainty of 15% produces 24% change in the $\Lambda_{Fe\text{-}Bm}$. (g) Laser spot size, r, changed by 15% (7.6 to 8.8 μm) has essentially no effect on the $\Lambda_{Fe\text{-}Bm}$. (h) Thermal conductance of Al/Fe-Bm interface and Al/silicone oil interface, G, has minimal effect on the $\Lambda_{Fe\text{-}Bm}$. Variation in the interface thermal conductance changes the slope of model fitting curve at longer delay time, typically longer than 1000 ps [*Cahill and Watanabe*, 2004; *Zheng et al.*, 2007]. A 10% uncertainty has already made the model fitting curve unable to fit the data well after 1000 ps. Thus the uncertainty in the interface thermal conductance is typically less than 10%, which propagates only 3% uncertainty in $\Lambda_{Fe\text{-}Bm}$.

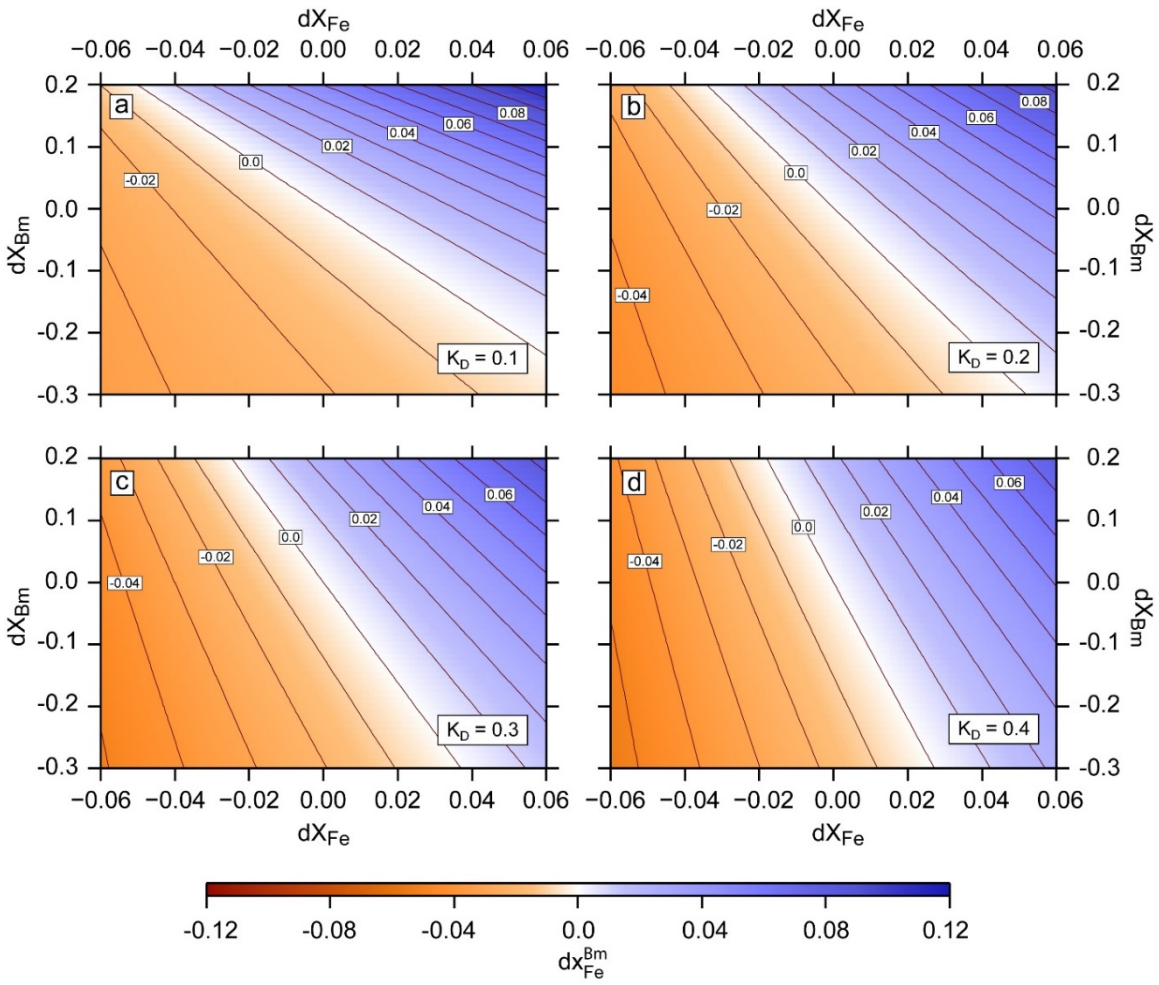

Figure S2. Variations in the iron fraction in bridgmanite, dx_{Fe}^{Bm}, as a function of variations in the global fraction of iron, dX_{Fe}, and volume fraction of bridgmanite, dX_{Bm}, and for four values of iron partitioning, K_D. The reference fractions of iron and bridgmanite are $X_{Fe,ref} = 0.09$ and $X_{Bm,ref} = 0.8$, and the reference iron fraction $x_{Fe,ref}^{Bm}$ as a function of K_D is shown by the brown curve in Fig. 4.

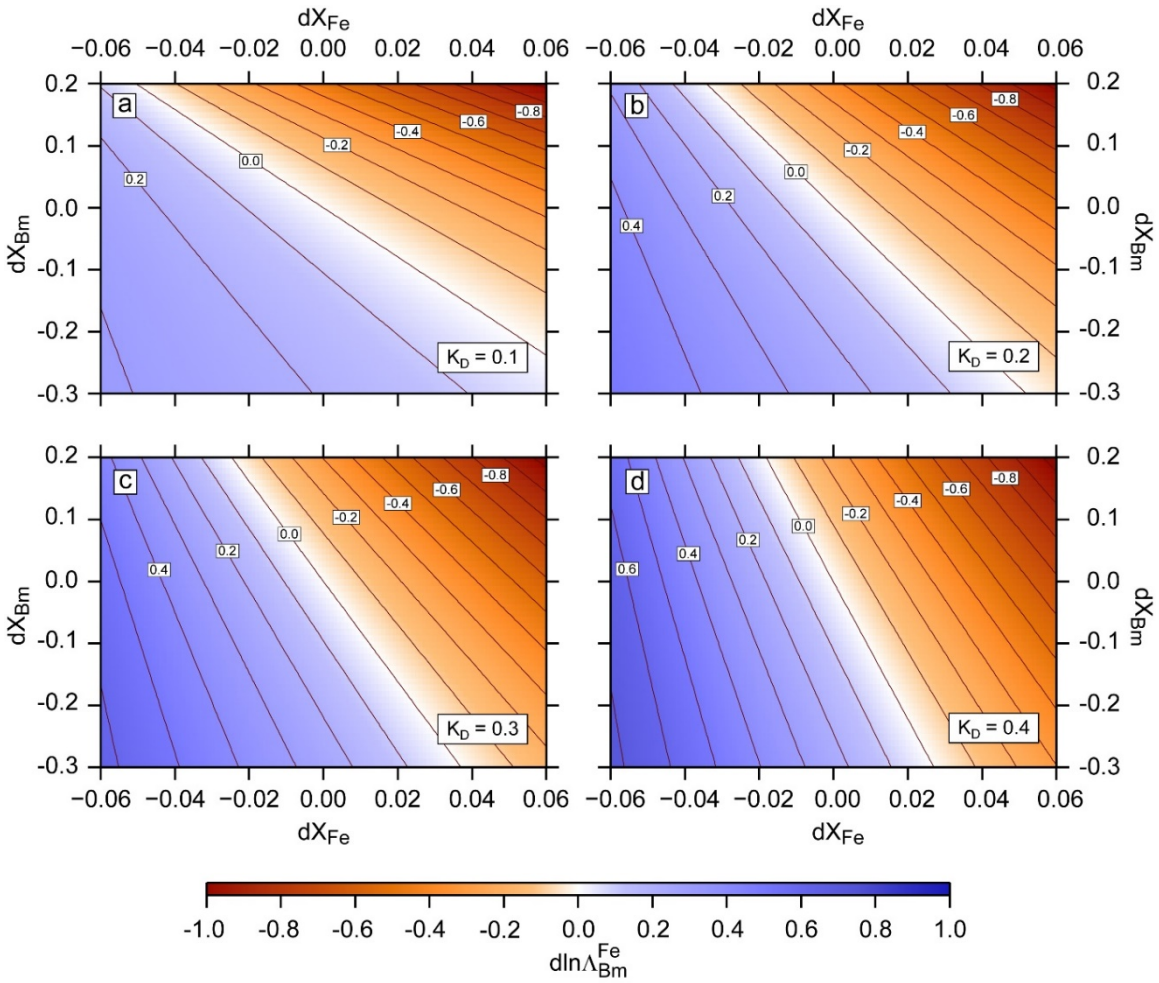

Figure S3. Relative variations in thermal conductivity of bridgmanite, $\mathrm{dln}\Lambda_{Bm}^{Fe}$, due to variations in the iron fraction (Eq. 4). Four values of the iron partitioning are shown, and results are plotted as a function of variations in the global fraction of iron, dX_{Fe}, and in the fraction of bridgmanite, with reference values, $X_{\mathrm{Fe,ref}}$ = 0.09 and $X_{\mathrm{Bm,ref}}$ = 0.8, respectively. The reference thermal conductivity depends on the iron partitioning and is represented by the dark blue curve in Fig. 4. Calculations are made at lowermost mantle pressure, P = 120 GPa, and a temperature of T = 3000 K.

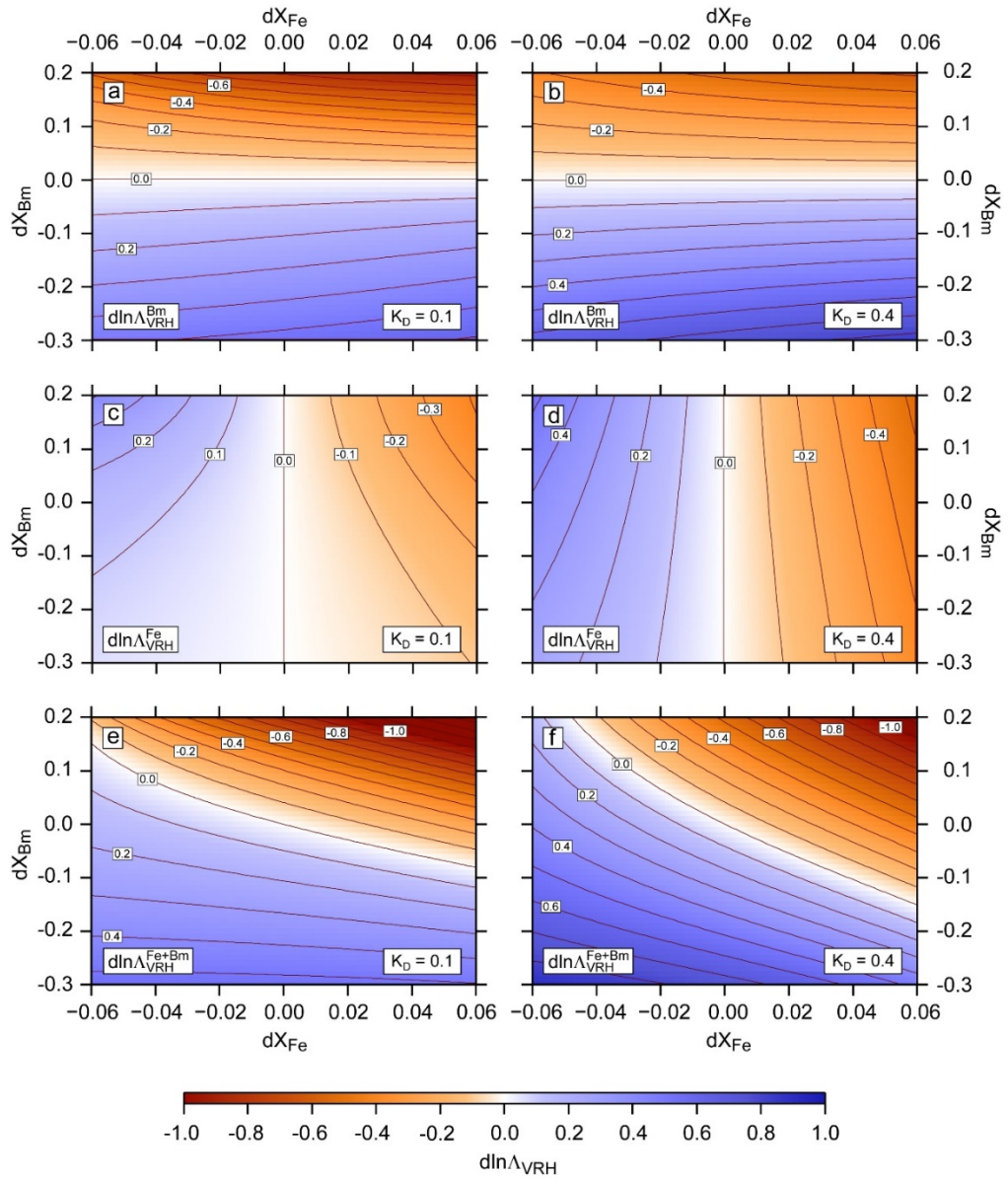

Figure S4. (a-b) Relative variations in thermal conductivity of mantle due to variations in the volume fraction of bridgmanite ($\mathrm{dln}\Lambda_{VRH}^{Bm}$, Eq. 8). (c-d) Relative variations in thermal conductivity of mantle due to variations in the global iron fraction ($\mathrm{dln}\Lambda_{VRH}^{Fe}$, Eq. 9). (e-f) Relative variations in thermal conductivity of mantle due to combined variations in volume fraction of bridgmanite and global iron content ($\mathrm{dln}\Lambda_{VRH}^{Bm} + \mathrm{dln}\Lambda_{VRH}^{Fe}$). In all cases, conductivity is estimated from the VRH average of an aggregate of bridgmanite and ferropericlase, and the conductivity of ferropericlase is assumed to be independent of the iron content. Two values of the iron partitioning are shown (K_D = 0.1, left column; and K_D = 0.4, right column), and results are plotted as a function of variations in the global fraction of iron, $\mathrm{d}X_{Fe}$, and in the fraction of bridgmanite, with reference values, $X_{Fe,ref}$ = 0.09 and $X_{Bm,ref}$ = 0.8, respectively. The reference thermal conductivity depends on the iron partitioning and is represented by the light blue curve in Fig. 4. Calculations are made at lowermost mantle pressure, P = 120 GPa, and temperature T = 3000 K.